Axial temperatures and electron densities in a flowing cascaded arc

AXIAL TEMPERATURES AND ELECTRON DENSITIES IN A FLOWING CASCADED ARC:

J.J. Beulens, M. de Graaf, G.M.W. Kroesen, and D.C. Schram,
University of Technology, Dept. of Physics,
P.O.Box 513, 5600 MB Eindhoven.

INTRODUCTION

Since about 1985 a cascaded arc is used as a particle source in the deposition machine described by Kroesen [1a,1b]. This method of deposition showed to be very fast and efficient to grow amorphous carbon films (a–C:H), varying from graphite and diamond to polymers [1,2]. The most important difference of this method, with respect to R.F. techniques, is that the three most important functions of a deposition process, as there are dissociation/ionization, transport and deposition are spatially separated. The dissociation takes place in a cascaded arc burning on argon. The temperatures in the arc are about 10000–12000 K. At the end of this arc hydrocarbons are injected which are then dissociated and ionized effectively. At the end of the arc the plasma expands supersonically into a vacuum vessel. That means that the plasma cools down and the formed hydrocarbon fractions are transported towards the substrate, where an amorphous carbon film can grow. The quality of the films depend mainly on the amount of energy available for each injected carbon atom. The behavior of the refractive index as a function of this energy could be a confirmation that in our deposition method the carbon ions rather than radicals govern the deposition process [1,3,4]. Therefore the cascaded arc is investigated numerically and experimentally in order to improve the ionization efficiency. The conservation laws for mass, momentum and energy for both the electrons and the heavy particles are solved 2 dimensionally by a control volume numerical method with a non staggered grid. By Fabry Perot interferometry heavy particle temperatures, electron temperatures and electron densities as a function of the axial position in the cascaded arc are measured. The obtained numerical results are compared to the experimental data, obtained by the optical Fabry Perot diagnostics.

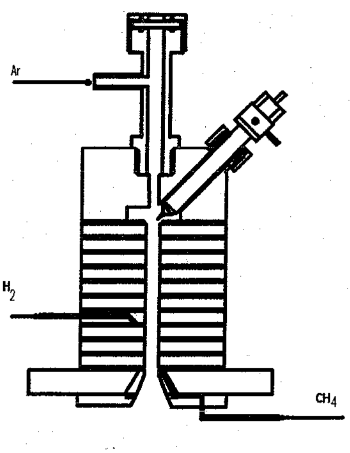

Fig.1 Outline of the cascaded arc as a particle source.

EXPERIMENTAL SET UP

The cascaded arc (fig.1) used in this work, consists of a stack of ten water cooled copper plates insulated electrically from each other by plastic (PVC) spacers and O–rings, three tungsten–thorium cathodes on one end and an anode on the other. Through the copper plates and the anode plate there is a bore of 4 mm diameter, forming a cylindrical channel of 6 cm long. The argon gas is fed through mass flow controllers and then injected at the cathode side. The gas or plasma is extracted through a nozzle in the anode plate which is mounted on a vacuum vessel. The pressure in the vessel is about 1 mbar, whereas the pressure in the arc is about 0.5 bar. This means that the plasma will be extracted supersonically. For the experiments the cascaded arc has two special features to measure the plasma pressure and to couple out the emitted light. The pressure is measured by a MKS baratron pressure transducer. The light is coupled out through an optical fiber and then coupled in an optical system (fig. 2). Between the two lenses L1 and L2 the light beam is parallel and thus a Fabry Perot interferometer can be placed here. The light source in figure 2 is a hollow cathode arc or a glow discharge on argon, to make a wavelength reference and to measure the apparatus profile. Lens L2 images the exit of the fiber on diaphragm D1. Finally, lens L3 images the diaphragm on the entrance slit of the monochromator (Jarrell–Ash 0.5 m). On the exit slit a photo multiplier is mounted. In the monochromator a 25 μm slit and a 50 μm slit were placed in order to obtain a trapezoidal monochromator apparatus profile with a flat part of 0.4 Å. The Fabry Perot interferometer in this experiment has a 1 mm spacing which gives a free spectral range of FSR=0.9 Å. By scanning the pressure in the Fabry Perot (1–4 bar argon, 1 FSR→ 0.8 bar) a spectral line can be scanned. The apparatus profile has a (FWHM) width of 15 mÅ.

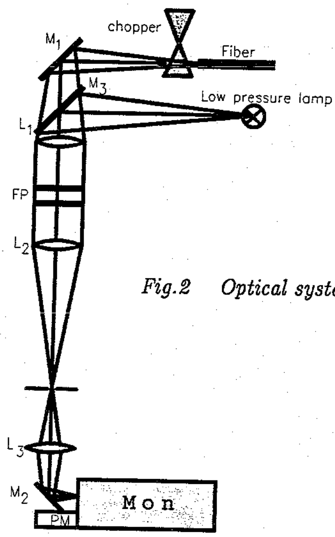

Fig.2 Optical system.

PLASMA DIAGNOSTICS

The wavelength dependent intensity profile of a spectral line emitted by the plasma is determined by several physical effects. Each effect can result in a shift of the line position and/or in a broadening of the line profile with usually either a Gauss or a Lorentz like contribution:

$$I_g(\omega) = \frac{1}{\Delta\omega_d\sqrt{\pi}} \exp\left[-\left(\frac{\omega-\omega_0}{\Delta\omega_d}\right)^2\right] \quad (1)$$

$$I_l(\omega) = \frac{\gamma}{2\pi}\frac{1}{(\omega-\omega_0)^2+(\gamma/2)^2} \quad (2)$$

where ω is the angular frequency, ω_0 the central resonance frequency, $\Delta\omega_d$ the width at $1/e^2$ of the top of intensity I_g and γ is the full width at 1/2 I_l. When more broadening mechanisms occur the line shape is in many cases a Voigt profile, which is a convolution of a Gaussian and a Lorentzian profile. In our case only the two mentioned mechanisms are dominant.

Doppler broadening gives rise to a gauss profile with width $\Delta\omega_d=(\omega/c)\sqrt{(2kT_h/m)}$ (at $1/e^2$), where k is the Boltzmann constant, m is the mass of the emitting particle, c is the speed of light and T_h is the heavy particle temperature. Also a shift of the central line occurs when there is a net velocity of the particles which makes an angle with the line of sight other than 90^0: $\Delta\lambda=-\lambda_0\cos\theta/c$, where $\Delta\lambda$ denotes the wavelength shift and λ_0 is the central undisturbed wavelength.

Another important broadening mechanism is Stark broadening. The quadratic Stark effect, which is the influence of charged particles on the energy levels of the emitting atom, give a Lorentz profile [5,6]. This stark effect gives for the (FWHM)width and shift respectively:

$$\gamma = N v^{1/3} C_4^{2/3} (\pi/2)^{2/3} \pi \tag{3}$$

$$\Delta = -\gamma/1.15 \tag{4}$$

were N is the density of the disturbing particle and C_4 a constant which value is about 10^{-22} $m^4 s^{-1}$ for neutral argon atoms. For hydrogen the profiles are not Lorentz like [5,6]. In case of hydrogen the (FWHM) width gives the electron density according to: $n_e = C(\Delta\lambda)^{3/2}$ in which C is a constant in the order of 1.2 10^{22} m^{-3} $nm^{3/2}$ (for Hβ and T= 1 eV).

The line/continuum ratio provides the electron temperature using the equation:

$$T_e = \frac{E_p}{k} \ln^{-1}\left[\frac{I_{\rm lijn}}{I_{\rm cont}}\right]_{\rm top} \frac{A_{pq} h c \lambda g_p \sqrt{T_e}}{4\pi\omega_i C_1 \Delta l n_e} \tag{5}$$

where ω_i is the partition function of the ArII system [7], g_p the statistic weight of the upper level and E_p the energy difference between the upper level p and the ion ground state, C_1=1.63 10^{-43} $Wm^4K^{1/2}sr^{-1}$ a constant, n_e the electron density and A_{pq} the transition probability from level p to q for spontaneous emission.

With the summed broadening effects we are able to determine both the heavy particle temperature and the electron temperature and also the electron density, when the line profiles are measured using a Fabry Perot interferometer and deconvoluted into Gauss and Lorentz parts. Note that the electron temperature T_e calculated from the line/continuum ratio is a LTE value.

MODEL

In accordance with the applications, a significant experimental and theoretical research work has been performed in this field, see [1,8,9]. However, it has been recognized that two–dimensional modeling of the processes in plasma torches is needed, [17,18], in order to treat correctly some phenomena such as highly non–isothermal flow, deviations from local thermodynamic equilibrium (LTE), as well as diffusion and heat conduction. In the present work a two dimensional model developed by Milojevic [10] is used to compare the experimental results with the numerical ones.

The model will be described here in a condensed way. In the approach adopted in the model the plasma is treated as a two–phase medium, which consists of heavy particles (neutral atoms and ions) and light particles (electrons). For the full description of this two–phase flow one needs to solve the mass, momentum and energy equations for both phases. However, due to the small electron mass, their momentum is neglected in comparison with the heavy particle momentum, and both phases are assumed to have the same convective velocity field. Therefore a two–phase flow character is kept only with respect to the heavy particle and electron temperatures which are assumed to be different and described by separate energy equations. Ohmic heat input is consumed by electrons, whose temperature increases, resulting in frequent elastic and inelastic collisions with the heavy particles, which are heated and ionized to higher and higher degree. The mass of the electrons is small and the elastic collisions are not always efficient enough to equalize the temperatures of the two phases, especially at inlet regions of the flow, where the cold gas is introduced, and in the vicinity of cooled walls.

The two–dimensional two–temperature model is developed for the predictions of a strongly flowing mono–atomic cascaded arc plasma. The flow is assumed to be axisymmetric, two–dimensional, compressible and strongly non–isothermal. The argon plasma is considered as singly ionized, locally quasi–neutral ($n_e \simeq n_i$) with local temperature non–equilibrium ($T_e \neq T_h$). The electric field is assumed to be one–dimensional, uniform over the arc cross–section ($E_r = 0$, $\partial E_x / \partial r = 0$). The total current is specified as an input parameter and is kept constant along the arc channel. equations. The system of 2 dimensional elliptic partial differential equations is solved by a control volume numerical method of Patankar and Spalding [11,12], extended by incorporating a non staggered grid approach of Peric [13] with momentum interpolation at control volume faces as suggested by Majumdar [14]. Density corrections from the equation of state are introduced into the pressure correction equation as proposed by Jensen [15], but with an additional upwind–like scheme. The system of algebraic discretization equations for each variable are solved by the strongly implicit 'SIP' procedure of Stone [16]. A numerical grid with 23x24 non–uniformly distributed points is used for all calculations. The calculations were performed on a IBM PC/RT.

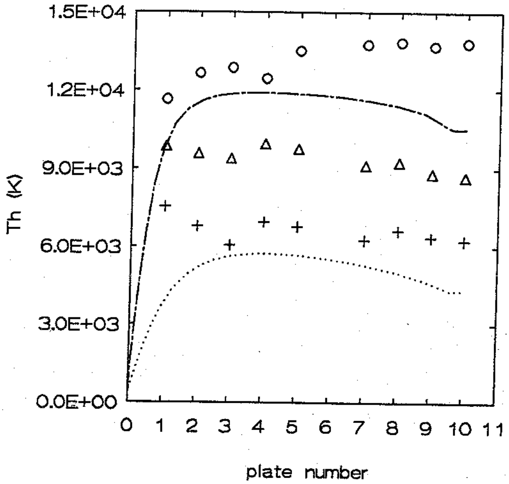

Fig.3 *Heavy particle temperature vs axial position and arc current for an argon flow of 50 scc/s. The lines are model calculations.* o, –.–.: *50 A*, Δ: *30 A*, +, ...: *20 A*.

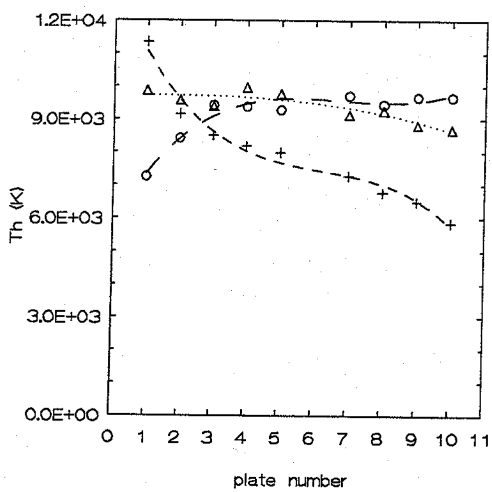

Fig.4 *Heavy particle temperature vs axial position and argon flow for an arc current of 30 A. The lines are fits through the experimental data.* o: *100 scc/s*, Δ: *50 scc/s*, +: *20 scc/s*.

RESULTS

In the experiments an argon ion line (435.4 nm) is used because the stark broadening of ion lines is about a factor of ten smaller than for neutral lines [5]. For our plasma this means that the stark width and the doppler width are of the same order of magnitude. The measured profiles are perfectly symmetrically and the width is of the order of 50 mÅ which consists of the Gaussian apparatus profile and about equal parts of the Doppler and Lorentz contributions. After deconvolution of the line profiles of the ArII–line (435.4 nm) the Gaussian part gives the heavy particle temperature T_h. The accuracy of the measured temperature is about 2%. Note that the measured temperatures (and electron densities) are not values at the axis of the arc, but an average over the cross section weighed on the detection efficiency and the density of the radiating particles versus the radial position. Nevertheless these values are close to the axial ones because of the higher ion density at the axis (higher line intensity) and a higher detection efficiency for the centre. In figure 3 the heavy particle temperature is plotted versus axial position and arc current. At low currents the plasma is heated fast and due to the expansion of the plasma the temperature is decreasing slowly. For higher currents the electrons need longer to heat the heavy particles and because the electron temperature T_e remains constant, see figure 5, a large deviation from thermal equilibrium is present. In figure 4 T_h is plotted versus axial position and flow rate at a current of 30 A. The lower the flow the faster the heating of the cold gas (plasma) at the inlet and the decrease of the temperature which partly can be due to the expansion of the gas and the higher power loss to the walls is higher for low flows. This means a lower power efficiency for lower gas flows. The electron density n_e, calculated from the Lorentz part of the measured line profile (equation 3), is plotted in figure 6. These for the electron density are in good agreement with the earlier measurements by Kroesen [1], who used H_β broadening of hydrogen 'impurities' in the arc. Comparing the experimental values of the temperatures, and the electron density with the modeled ones they show the same trend and the absolute values differ less than 25%. Only the low flow settings are not yet modeled correctly to fully understand the behavior of the arc at these settings.

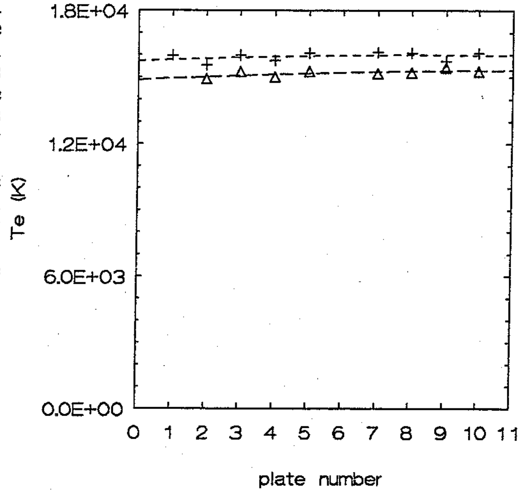

Fig.5 *Electron temperature vs axial position and argon flow for an arc current of 50 A. The lines are fits through the experimental data. □ : 50 scc/s, +: 100 scc/s.*

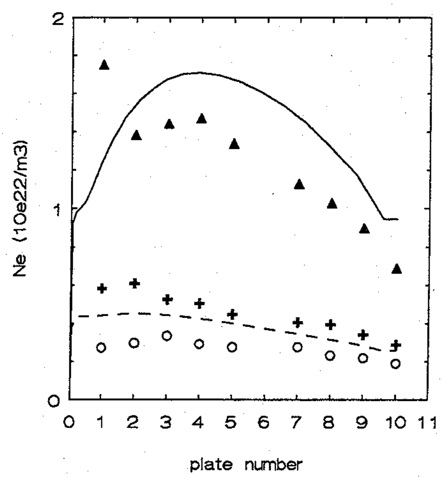

Fig.6 *Electron density vs axial position and arc current for an argon flow of 50 scc/s. The lines are model calculations. ▲, ______: 50 A, +: 30 A, o,– – – –: 20 A.*

CONCLUSIONS

The used Fabry Perot interferometry diagnostic shows to be a very good tool for measuring temperatures and electron densities in a flowing cascaded arc with an accuracy of about 2%. Only one line profile needs to be measured to obtain T_e, T_h and n_e. The numerical results are already quite close to the experimental ones and can be used to predict the behavior of the arc plasma at least for the parameters on and near the axis. Further research needs to be done to close the gap between the experiment and the model by measuring in two dimensions and by improving the model. The model can be improved for example by including radiation transport in a more refined way and by using a two dimensional current density, and thus electric field.

REFERENCES

[1a] Kroesen G.M.W., PH. D. thesis, University of Technology Eindhoven, the Netherlands (1988).
[1b] Kroesen G.M.W., Schram D.C., de Haas J.C.M., Description of a flowing cascade arc plasma, to be published.
[2] Bachmann P.K., Beulens J.J., Kroesen G.M.W., Lydtin H, Schram D.C. and Wiechert D.U., proceedings of the TMS conference, aug.28–sept.1 1989.
[3] Savvides N. and Window B., J. Vac. Sci. Technol. A3, 2386, 1985.
[4] Savvides N., J. Appl. Phys. 59,4133,1986.
[5] Griem H.R.,"Spectral line broadening by plasmas", Academic press, New York, USA(1974).
[6] Sobel'man, "Introduction to the theory of atomic spectra", Pergamon press, Oxford (1972)
[7] Drawin H.W. and Felenbok P., "Data for plasmas in LTE", Gauthier–Villars, Paris(1965).
[8] C.J. Timmermans, R.J. Rosado and D.C. Schram, Z. Naturforschung 40A(1985)810.
[9] J.C.M. de Haas, Ph. D. thesis, University of Technology Eindhoven, the Netherlands (1986).
[10] D. Milojevic, A two dimensional model for flowing cascaded arc plasma, to be published.
[11] S.V. Patankar and D.B. Spalding, Int. J. Heat and Mass Transfer 15(1972)1787
[12] S.V. Patankar, 'Numerical Heat transfer and fluid flow', McGraw Hill, NY USA (1980)
[13] M. Peric, R. Kessler and G. Scheurer, 1987 University Erlangen–Nurnberg, Lehrstuhl fur Stromungsmechanik, Report LSTM 163/T/87.
[14] S. Majumdar, Numerical Heat Transfer 13(1988)125.
[15] D.E. Jensen, D.B. Spalding, D.G. Tatchell and A.S. Wilson, Combustion and Flame 34(1979)309.
[16] H.L. Stone, SIAM J. Num. Anal. 5(1968)530.
[17] J. Mostagimi, P. Proulx and M.I. Boulos, Numerical Heat Transfer 8(1985)187.
[18] J. Mostagimi, P. Proulx and M.I. Boulos, J. Appl. Phys. 61(1987)1753.